ORIGINAL ARTICLE

Classification algorithm for thyroid scan disorders; a computer aided diagnostic approach to get a second opinion for thyroid abnormalities

Abdul Qayyum[1], Muhammad Shahban[2*], Noor Nissa Qureshi[1], Quratulain Soomro[1]

Pakistan Journal of Nuclear Medicine
Volume 11(1):15–21
https://doi.org/10.24911/PJNMed.175-1590377862

Pakistan Journal of Nuclear Medicine is the official journal of Pakistan Society of Nuclear Medicine

ABSTRACT

Background: The thyroid is one of the largest and most important glands in the endocrine system. It controls cellular metabolism by releasing hormones directly into the bloodstream. However, thyroid hormone disorder may lead to depression, fatigue, memory loss, and much more. Therefore, in order to assess thyroid disorder, gamma scintigraphy is extensively used to diagnose the malfunction of the thyroid. The current study proposed a simple computer-aided diagnosis technique to detect any nodular abnormalities in the thyroid.

Methods: The proposed technique involves suppressing noise in thyroid scans, segmentation of thyroid glands from the Technetium-99m (^{99m}Tc) scan, and the use of an support vector machine classifier to classify thyroid scan into normal and abnormal based on the extracted features. The local binary pattern technique was employed to extract features of normal and nodular thyroid scans.

Results: Performance of classifiers was optimized in such a way that areas under the curve of receiver operative curve was maximized.

Conclusion: An easy-to-use graphical user interface was developed for the validation of the proposed technique on the NORIN thyroid database which gave results with an accuracy of 92%.

Keywords: CAD, AUC, ROC, MATLAB in nuclear medicine, thyroid scintigraphy, binary masking, image feature extraction.

Received: 25 July 2020 **Revised:** 10 May 2021 **Accepted:** 15 May 2021

Correspondence to: Muhammad Shahban
*Atomic Energy Cancer Hospitals NORI, Hanna Road, Islamabad, Pakistan.
Email: shahban_butt@yahoo.com
Full list of author information is available at the end of the article.

Introduction

Thyroid is the largest gland in the endocrine system that has a high influence on the functioning of other body functions. Its essential function is to synthesize, store, and secrete iodinated hormones, which are essential for cellular metabolism. It is made up of two pear-shaped lobes on either side of the trachea. These lobes are connected by a small tissue called the isthmus giving it a whole shape of a butterfly [1-3]. Measurement or assessment of thyroid function is one of the oldest use of nuclear medicine diagnostics techniques [4]. Although ultrasound imaging of thyroid and thyroid cytology are extensively used for diagnosis of thyroid disorders, thyroid scintigraphy is a vital tool used for decision making regarding thyroid functionality and subsequent thyroid therapy [5]. Previously, Iodine-131 (^{131}I) was used for thyroid scintigraphy. However, high patient dose (due to high energy gamma and beta emission) and need of high energy collimation (for the photon energy of 364 keV and above) made ^{131}I less favorable and is largely replaced by ^{123}I and Technetium-99m (^{99m}Tc). Since both of these isotopes carry low photon energy, best suited for scintigraphy, and hence result in comparatively lower patient dose. In most nuclear medicine departments, ^{99m}Tc is preferred over ^{123}I due to its cost-effectiveness, lower dose, and easy availability [5]. When ^{99m}Tc activity is injected into the patient's body, a portion of the activity is absorbed in thyroid glands. ^{99m}Tc scans are performed after 20-30 minutes of injection [6]. The clinical presentation of thyroid disease falls into two broad categories; those associated with an alteration of thyroid functional status with or without distorting the shape and secondly those with distorted anatomy (enlarged with or without nodules) without an initial alteration in thyroid functional status. In both situations, a thyroid scan makes an important contribution to the diagnosis and management of the condition. The status of thyroid nodules can be identified from gamma scan while thyroid abnormalities representing

malfunctioning of thyroid cannot be easily identified from a scan (however radioactive iodine uptake has a role in it). A further clinical and pathological examination may be required to assess either the condition of tumor/nodules (benign and malignant) or identification of hyper/hypothyroidism [7]. A careful interpretation of thyroid scan; in conjunction with patient history, clinical examination, ultrasound imaging, and thyroid function test is vital in an effective diagnosis of thyroid disorder. Ultrasound test is, sometimes, complimented with thyroid scintigraphy for better diagnosis. Some types of thyroid abnormalities can easily be identified solely from the gamma images, i.e., hot or cold nodules and multinodular goiter. An abnormal thyroid image especially that of nodular thyroid is, sometimes, very difficult to read and delineate because of vague boundaries merged with surrounding tissues [8] in which case our proposed technique may provide a second opinion to radiologists and could enhance sensitivity to detect lesions. Computer-aided diagnosis (CAD) through image processing has a potential role in the detection of cold and hot nodules from a thyroid scan (cold nodules has higher chances of malignancy in comparison to hot nodules). CAD techniques are continuously being developed and improved for better diagnosis of diseases from diagnostic images. Previously Marko et al. [9] developed a matrix laboratory (MATLAB) tool for tumor detection in ^{99m}Tc scintigraphy. In that study, Gamma images were acquired from a single photon emission computer tomography system. Afterward, the region of interest (ROI) around thyroid gland is manually cropped from thyroid scans and then a combination of edge detection and morphological operation techniques were employed to detect the exact boundary of the thyroid glands. Later on, a correlation filter was developed to detect any tumor-based abnormalities in the thyroid glands. The beauty of this technique is that it is simple and easy for tumor detection; however, there are some limitations to this technique, i.e., it was not a fully automated method, since radiologist would require manual cropping of the thyroid glands; second, the performance of edge detection techniques is compromised in the presence of background noise as high background noise is a usual case in scintigraphy and last, the dataset used in this methodology is very small as entire methodology was developed on 20 scintigraphy images. The present article addressed the limitations faced by Marko et al. [9] as the proposed methodology is completely automated. The segmentation process is improved by eliminating background noise and a larger database of 250 thyroid scans, as compared to 20 patiens in previous study, was used in this study.

Materials and Methods

In this study, a total of 250 patients were randomly selected, who came for thyroid scintigraphy. The whole study was conducted in two phases. In the first phase, a team of nuclear physicians analyzed these scans through visual interpretation along with clinical and pathological data and categorized the images into two main groups as follows: one contains the images of patients having appearances of nodules, i.e., hot/cold nodules and multinodular goiter, irrespective of their functional status and is called group A; the other constitutes images of either normal patients or patients of diffuse goiter irrespective of their functional status and designated as group B as shown in Figure 1. In the second phase, an algorithm was designed to categorize thyroid scan into group A and group B on the basis of image processing using MATLAB program. First of all median filtering is employed to remove scale, patient name, patient ID, etc. from thyroid scan. In the second step, an average value of background pixel is calculated to binaries given thyroid scan as described in step 3. Later on, morphological image reconstruction techniques were employed to reconstruct noise removed binary thyroid gland image as indicated in step 4. Finally, the thyroid gland is constructed in step 5 by multiplying binary thyroid gland obtained in step 4 with the original thyroid scan. After successful segmentation of thyroid gland, local binary pattern (LBP) features are extracted from ROI and finally, a kernelized support vector machine (SVM) based classification was adopted for identification of cold and multi-nodules in a given thyroid scan. Detail of every step is discussed below as shown in Figure 2.

Median filtering

Noise suppression in digital thyroid scans is an important step in CAD techniques for detection and classification of thyroid malignancies [10]. Figure 3 shows that, in addition to thyroid glands, some unnecessary information like patient name, ID, date of birth, image resolution, image

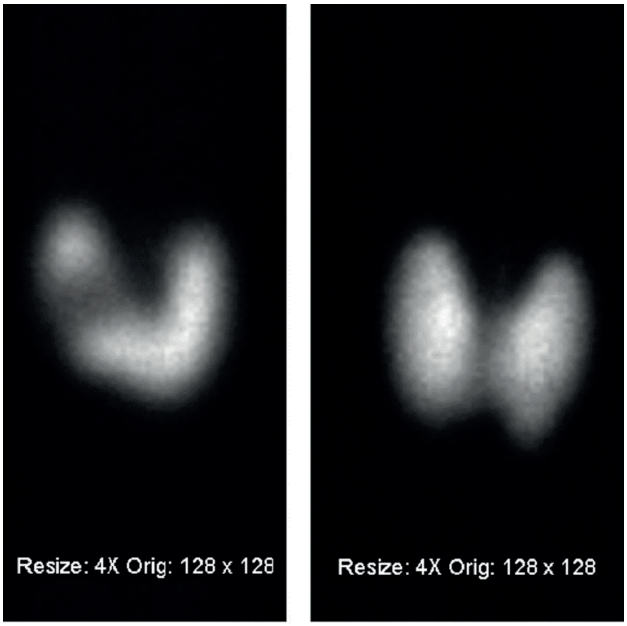

Figure 1. *Figure on the right is an example of thyroid scans of group A while the image on the right represents group B.*

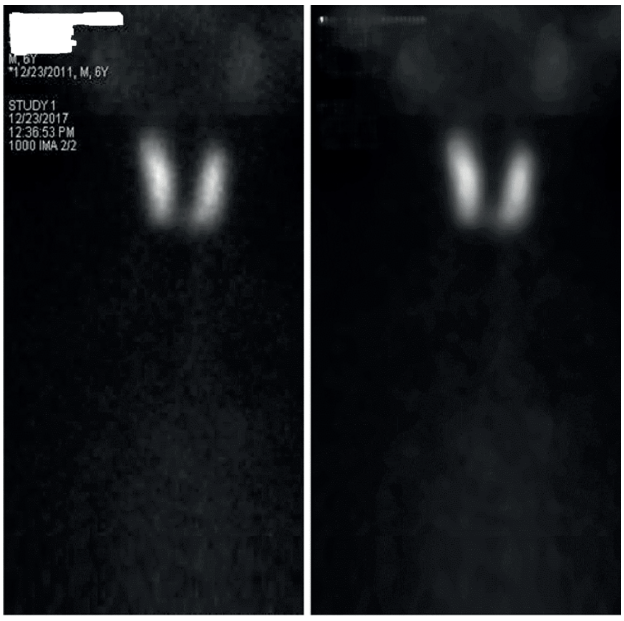

Figure 2. *Before (left) and after(right) the application of the median filter.*

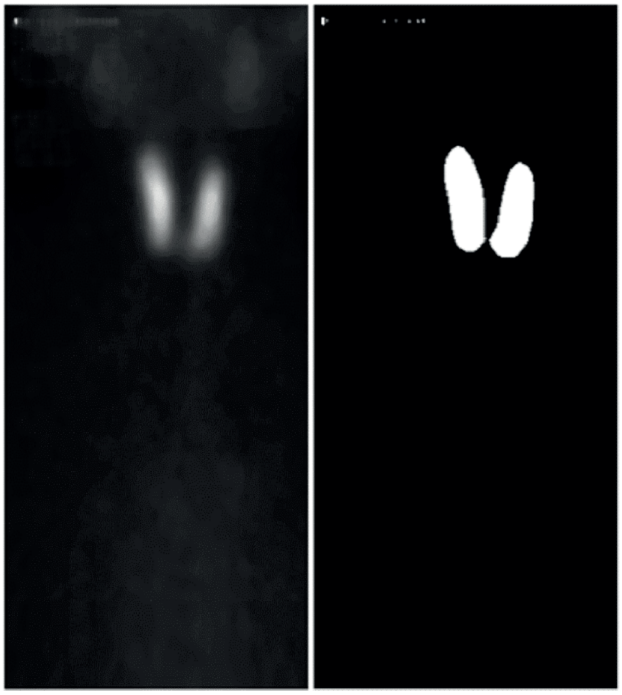

Figure 3. *Binary masking of gamma scan which eliminated background noise.*

scale are also included in a scintigraphy scan. Similarly, a thyroid scan may also include high background noise around thyroid lobes. Therefore, it is necessary to suppress background noise and other unnecessary information from thyroid scans. For this purpose, a non-linear median filter was used in such a way that for every pixel, a 11 × 11 neighborhood is considered as a center. In median filtering, the value of the pixel is replaced by the median of the pixel values in the 11 × 11 neighborhood. The superiority of non-linear median over a linear filter is that it doesn't spread noise along its neighbor and preserves edges [11-13]this folk-theorem is seen to be false in general. We show that median filtering and linear filtering have similar asymptotic worst-case mean-squared error (MSE. Original gamma scan before applying the median filter and resulting output is shown in Figure 3.

Binary mask generation by eliminating background noise

Several image segmentation techniques have been proposed in the literature, however, adaptive thresholding and Otsu's segmentation technique are two major techniques used for image segmentation [14,15]. Both of these techniques have their pro & cons, such as in Otsu's segmentation it is supposed that there are two separate pixel intensity distributions for foreground and background in image histogram. However, the presence of background noise in thyroid scans makes it difficult to distinguish foreground from background accurately. Similarly, adaptive thresholding is not useful in the presence of uniform background noise, which is an obvious case in thyroid scans. Therefore, efficient segmentation of thyroid glands is very difficult to achieve through adaptive or Otsu'segmentation techniques. One way to achieve effective segmentation is to estimate the average intensity value of background noise. Since thyroid glands are the brightest objects in the image, therefore, it could be assumed that all high-intensity values in the image belong to thyroid glands and low-intensity values belong to background noise pixels. Let's denote any pixel in an image by $I(x,y)$ and background pixel by $I_b(x,y)$, then all of the possible candidate pixels for background are estimated as,

$$I_b(x,y) = \begin{cases} I(x,y) & ; \quad \text{if } 0 < I(x,y) < 0.25 \times I\text{max} \\ 0 & ; \quad \text{otherwise} \end{cases}$$

where, $I_b(x,y)$ is the intensity of pixals as shown in Figure 3 and I_{max} is the maximum intensity in the image. Above equation assumes that every non-zero pixel whose intensity level is less than 25% of I_{max} is a possible candidate to be a background pixel.Afterward, estimation of the background was carried out by calculating an average value of every non-zero pixels in Image $I_b(x,y)$. Let's denote this average value by , which was used to binaries entire thyroid scan. The result of binary segmentation is shown in Figure 3.

$$I_{bw} = \text{Imbinaries}(I > 2.5 \times I_{bAvg})$$

where, I_{bw} is the binary mask of thyroid scans.

Image reconstruction

Extraction of thyroid gland in binary mask

In addition to thyroid glands, binary mask obtained in the previous step contains other small objects. It is necessary to remove unnecessary objects for reconstruction of thyroid glands. For this purpose, different morphological image processing techniques are employed. From Figure

3(a), it is clear that maximum intensity pixels lie within thyroid glands; therefore, the location of any of these pixels could be set as Marker point in morphological image reconstruction. Coordinates of Marker in an image I_b can be found by following MATLAB command:

$$[x_{cor}, y_{cor}] = \text{find}(I_b = \max(I_b(:)))$$

where x_{cor} and y_{cor} are the coordinates of Marker.

Figure 4(b) shows the automatically generated Marker image at coordinates, and Figure 4(c) shows extraction of a thyroid gland by using Marker of Figure 4(b) and mask image Figure 4(a). Limitation of this algorithm is being indicated in Figure 4(c) as only one lobe of thyroid gland could be extracted, because of the reason that two lobes of thyroid gland were not interconnected. Therefore, we needed to extract the remaining lobe of the gland. For this purpose, a centroid of Figure 4(c) is calculated using built-in Matlab function "centroid (Image)."

A fixed size Marker is constructed that passes through the centroid as indicated in Figure 4(e). Finally, Figure 4(f) indicates extraction of the complete thyroid gland by using Marker in Figure 4(e) and Mask in Figure 4(a) by morphological image reconstruction technique.

Complete thyroid gland extraction

Once the thyroid extraction is completed in a binary mask, the next step was to extract thyroid gland from the original thyroid scan. The algorithm used to extract thyroid gland is as follows:

1. Enclose thyroid glands in Figure 4(f) into a rectangle as shown in Figure 5(a).
2. The hole-filling algorithm [16] was employed in Figure 5(a). The result of hole-filling is shown in Figure 5(b).
3. Finally, complete extraction of thyroid glands is achieved by pixel-wise multiplication of image in Figure 5(b) with Figure 5(c). Figure 5(d) shows complete extraction of the thyroid gland.

Feature extraction

Just after the successful extraction of thyroid glands, a thyroid scan is ready for further processing, i.e., for the detection of nodules. Nodule detection from image starts with the feature extraction from normal and nodular thyroid scans. Several feature extraction techniques have been proposed in literature i.e. Gabor features, gray level co-occurrence matrix etc. [16-18]. However, proposed methodology used LBP feature extraction technique. LBP features extraction was carried out from 200 thyroid scans, in which 70 were normal and 130 were cold or multi-nodular scans. Feature vector obtained through LBP entirely depends on size of thyroid glands [19]. In order to limit the size of feature vectors, all of the thyroid scans were resized to 200 × 200 matrixes. Furthermore, in order to extract more localized features, thyroid image is further sub-divided into four regions R1, R2, R3, and R4. LBP features were extracted separately from each individual region. LBP feature vectors were computed by using MATLAB code [20] and the length of the LBP feature vector is calculated as

$$\text{LFV} = N^2 \times ((P \times (P-1)) + 3)$$

Where LFV is the length of a feature vector, P is the number of regions, is the number of neighbors used to compute LBP.

Substituting $N = 4$, $P = 4$ in the above equation, the length of feature vector comes out to be 1 × 240. Size of feature vector was varied by varying parameters in the above equation.

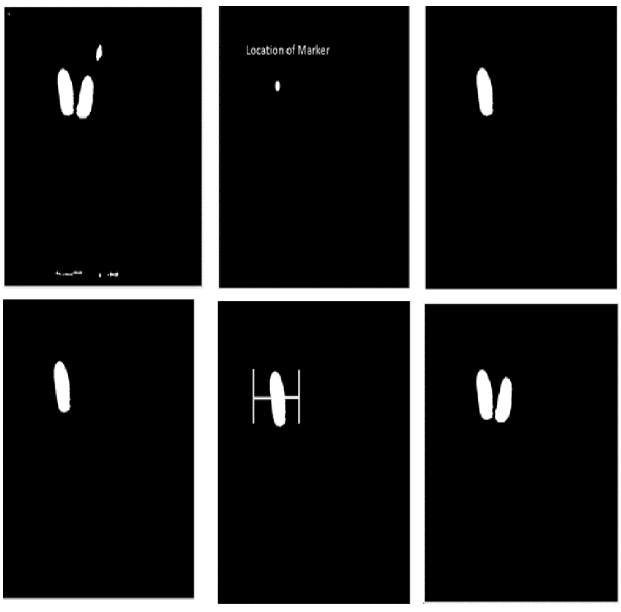

Figure 4. *Step by step procedure of thyroid extraction.*

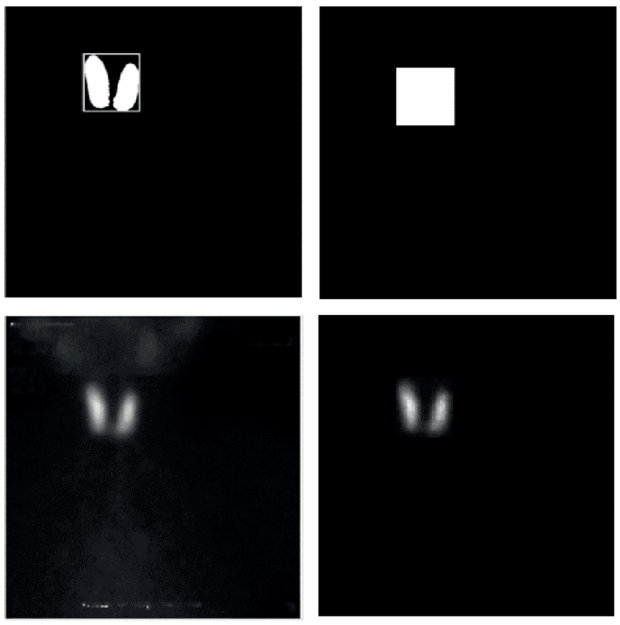

Figure 5. *Complete thyroid gland extraction.*

Training classifier

LBP features obtained in previous steps were classified using SVM. SVM uses linear discriminant function to classify features into two or more different classes with a linear separator in a feature space. Assume the feature space is *m* dimensional, then the separator would be a hyper plane of *m*-1 dimensions. Mathematically, linear discriminant function of SVM is represented as,

$$f(\boldsymbol{x}) = \mathbf{sgn}\ (\boldsymbol{w}^T\boldsymbol{x} + b)$$

where

$$\boldsymbol{w}^T\boldsymbol{x} = \sum_{j=1}^{m} \mathrm{w_j x_j}$$

$\boldsymbol{x}_j$ is a feature vector of *jth* example,
$\boldsymbol{w}$ is a weight vector and
b is a biased value.

Here **sgn** function returns +1 labels if its argument is greater than 0, otherwise it returns -1 for argument less than 0. In SVM and are adjusted such that, following criteria is satisfied.

$$\mathbf{min}\ \eta = \frac{1}{2}\boldsymbol{w}^T\boldsymbol{w}$$

s. t,

$$\boldsymbol{w}^T\boldsymbol{x_i} + b \leq -1, \qquad \forall i\ s.t\ \mathrm{y_i} = -1$$

$$\boldsymbol{w}^T\boldsymbol{x_i} + b \geq -1, \qquad \forall i\ s.t\ \boldsymbol{y_i} = +1$$

Here, $\boldsymbol{y}$ represents output label. SVM classifier is robust and finds an optimum boundary between positive and negative class features. In the current research, SVM toolbox of MATLAB 2016 (a) was employed for classification of normal and abnormal thyroid scans. Since LBP features obtained in the previous step were linearly non-separable, therefore, kernelized SVM was trained with second order polynomial degree. Finally, kernelized SVM classifier is optimized in such a way that area- under-curve (AUC) of receiver operative curve (ROC) was maximized.

Selection of Database

Locally available data of our hospital were selected for the validation of above-mentioned methodology. This database contains all possible forms of thyroid scans. This database consisted of total 200 thyroid scans (one thyroid scan per patient). Each thyroid scan was digitally stored at a spatial resolution of 512 × 512 pixels with 0-255 gray scale levels. At first, a team of experienced radiologists and medical doctors categorized the entire database into two major categories, i.e., normal and abnormal scans. There were 70 patients whose scans were found normal and 130 were abnormal. Among abnormal patient scans, all abnormalities like hot nodules, cold nodules, multinodular, hypothyroidism and hyperthyroidism were present. A classifier was trained on this database. Performance of classifier was evaluated by AUC value obtained from the ROC curve. ROC curve for trained SVM classifier is in Figure 6. AUC value for given ROC curve comes out to be 0.9788.

Graphical User Interface (GUI)

A GUI is worked out to make this program easy to use for radiologists. GUI essentially consists of three buttons; namely load image, segment image, and

image status. By using load image, any thyroid scan can be loaded in GUI. Window on the left side of GUI displays selected image. “Segment image” button basically displays only thyroid images automatically cropped from the whole scan. Image status button provides final results of the whole process that the image is either normal or abnormal as shown in Figure 7.

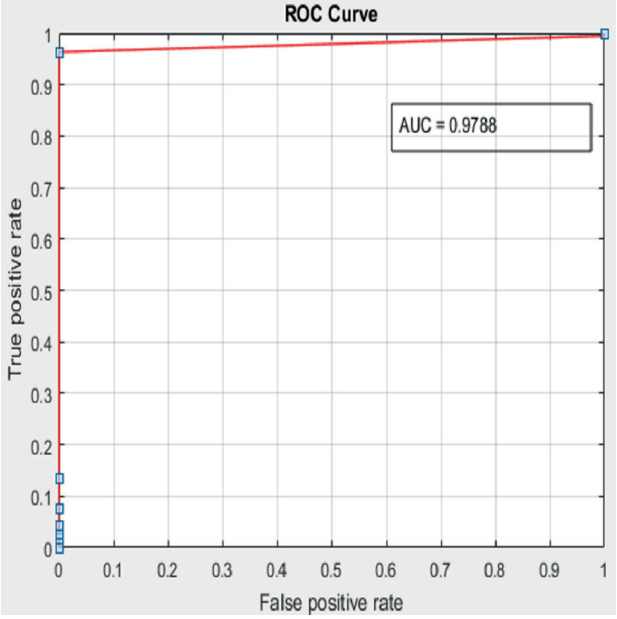

Figure 6. *ROC curve of classifier.*

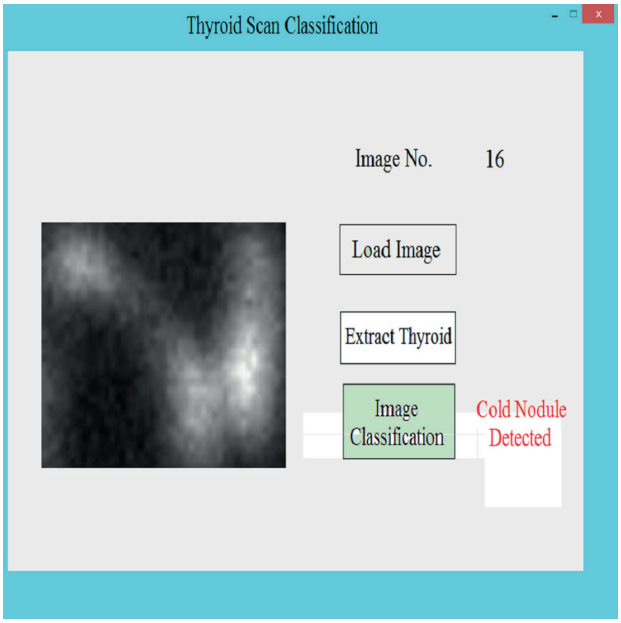

Figure 7. *GUI with a loaded image for nodule detection.*

Table 1. *Results of classification measures for classifier trainer.*

Classification measures	Value
True positive	18%
True negative	28
False positive	20%
False negative	20%
Accuracy	92%
Error	8%
Sensitivity	90%
Specificity	93%
f-value	0.91%

Results

Proposed algorithm was tested on 50 thyroid scans in which 20 scans were abnormal (containing either cold or nodular abnormalities) while 30 scans were normal (without containing any nodular abnormality). Results of classifier are summeraized in Table 1.

Discussion

Results of proposed algorithm is shown to expert radiologists and medical doctors. This team carefully observed the results of our classifer and then validated following findings, i.e., out of 20 abnormal scans, proposed algorithm was able to classify 18 abnormal scans successfully and similarly 28 out of 30 normal scans were classified correctly and hence achived accuracy upto 92%. Sicnce the precession, recall value are also comparable thus, it can be established that proposed methodology can be employed to detect abnormalities within thyroid scans.

Conclusion

Thyroid gamma scintigraphy is the oldest use of nuclear medicine imaging which is used to check thyroid performance in conjunction with lab tests and ultrasound imaging. MATLAB is a useful tool to design and use computer applications to classify thyroid gamma scans into normal and abnormal scans. LBP technique was used to extract key features of thyroid images which are then used to classify thyroid scans into normal and abnormal scans. A classifier was trained on 150 thyroid scans which were then used to detect/classify 50 thyroid scans into normal and abnormal thyroid scans. MATLAB program, based on the proposed methodology successfully classified all gamma scans with a success rate of 92%. This study can be extended further to classify abnormal scans into hot/cold nodules and multinodular goiter based on the same classification technique. A database of at least 1,000 images will be required for this purpose.

Pertinant findings

A simple CAD technique was proposed to detect any nodular abnormalities in thyroid. The proposed technique compares certain features of thyroid scan with alreadty stored database and classify gamma scan on the bases of those features into normal and nodular thyroids.

Implication for patient care

A GUI based application was designed using MATLAB which can be used by the physician to get a second opinion for thyroid classification.

List of Abbreviations

AUC	Area under the curve
CAD	Computer aided diagnostic
LBP	Local binary pattern
MSE	Mean square error
ROC	Receiver operative curve
ROI	Region of interest
SPECT	Single photon emission computer tomography
SVM	Support vector machine

Conflict of interest

The authors declare that there is no conflict of interest regarding the publication of this article.

Funding

None.

Consent to participate

This research is based on retrospective data. No patient information is disclosed in the article so consent was not signed from the patients

Ethical approval

Not Applicable.

Author details

Abdul Qayyum[1], Muhammad Shahban[2], Noor Nissa Qureshi[1], Quratulain Soomro[1]

1. NORIN Cancer Hospital, Sakrand Road, Nawabshah, Pakistan
2. Atomic Energy Cancer Hospitals NORI, Hanna Road, Islamabad, Pakistan

References

1. Heena GK. A review paper on various segmentation methods used on ultrasound images for thyroid diagnosis. Int Res J Eng Technol. 2017;4(6):836–9.
2. Sundaraiya S. Nuclear imaging in thyroid diseases - an overview. Chennai, India: SM Group; 2016.
3. Van De Graaff KM. Human Anotomy. 6th ed. New York, NY: The McGraw-Hill; 2001.
4. Bailey DL, Humm JL, Todd-Pokropek A, van Aswegen A. Nuclear medicine physics: a handbook for teachers and students. Vienna, Austria: IAEA; 2014.
5. Biersack HJ, Freeman LM. Clinical nuclear medicine. Berlin, Heidelberg: Springer; 2007. https://doi.org/10.1007/978-3-540-28026-2
6. Ziessman HA, O'Malley JP, Thrall JH. Nuclear medicine. 3rd ed. Philadelphia, PA: Mosby; 2006. https://doi.org/10.1016/B978-0-323-02946-9.50006-4
7. Mendre W, Raut RD. Thyroid disease diagnosis using image processing: a survey. Int J Sci Res Publ. 2012;2(12):1–4.
8. Koundal D, Gupta S, Singh S. Computer-aided diagnosis of thyroid nodule: a review. Int J Comput Sci Eng Surv. 2012;3(4):67–83. https://doi.org/10.5121/ijcses.2012.3406

9. Marko D, Jankovic MM, Koljevi-Marković A. A Matlab tool for tumor localization in parathyroid sestamibi scintigraphy. Telfor J. 2015;7(2):103–7. https://doi.org/10.5937/telfor1502103D
10. Qayyum A, Basit A. Automatic breast segmentation and cancer detection via SVM in mammograms. Int Conf Emerg Technol. 2016;1–6. https://doi.org/10.1109/ICET.2016.7813261.
11. Arias-Castro E, Donoho DL. Does median filtering truly preserve edges better than linear filtering? Ann Stat. 2009;37(3):1172–206. https://doi.org/10.1214/08-AOS604
12. Hamza AB, Luque-Escamilla PL, Martínez-Aroza J, Roldán RR. Removing noise and preserving details with relaxed median filters. J Math Imaging Vis. 1999;11(2):161–77. https://doi.org/10.1023/A:1008395514426
13. Koo JI, Park SB. Speckle reduction with edge preservation in medical ultrasonic images using a homogeneous region growing mean filter (HRGMF). Ultrason Imaging. 1991;13(3):211–37. https://doi.org/10.1177/016173469101300301
14. Verma OP, Hanmandlu M, Susan S, Kulkarni M, Jain PK. A simple single seeded region growing algorithm for color image segmentation using adaptive thresholding. Int Conf Commun Syst Netw Technol. 2011;500–3. https://doi.org/10.1109/CSNT.2011.107
15. Ghaye J, Kamat MA, Corbino-Giunta L, Silacci P, Vergères G, De Micheli G, et al. Image thresholding techniques for localization of sub-resolution fluorescent biomarkers. Cytometry A. 2013;83(11):1001-16. https://doi.org/10.1002/cyto.a.22345
16. Zhao H, Chen ZX. A simple hole filling algorithm for binary cell images. Appl Mech Mater. 2013;433–5:1715–9. https://doi.org/10.4028/www.scientific.net/AMM.433-435.1715
17. Tou JY, Tay YH, Lau PY. Gabor filters and gray level co-occurrence matrices in texture classification [Internet]. Princeton, NJ: Citeseer; 2007 [cited 2021 May 20]. pp 197–202. Available from: https://citeseerx.ist.psu.edu/viewdoc/download?doi=10.1.1.140.4766&rep=rep1&type=pdf#:~:text=The%20Grey%2Dlevel%20Co%2Doccurrence,techniques%20used%20on%20texture%20classification.&text=The%20experiments%20showed%20that%20the,features%20decomposed%20to%20six%20features
18. Mirzapour F, Ghassemian H. Fast GLCM and gabor filters for texture classification of very high resolution remote sensing images. Int J Inf Commun Technol Res. 2015;7:21–30.
19. Guru DS, Kumar YHS, Manjunath S. Textural features in flower classification. Math Comput Model. 2011;54(3–4):1030–6. https://doi.org/10.1016/j.mcm.2010.11.032
20. Mathworks support: extract LBPFeatures [Online]. Available from: https://www.mathworks.com/help/vision/ref/extractlbpfeatures.html